

1 **UV grafting: surface modification of cellulose nanofibers without the use of**

2 **organic solvents**

3 Xianpeng Yang*, Ting-Hsuan Ku, Subir K. Biswas, Hiroyuki Yano and Kentaro Abe*

4 Research Institute for Sustainable Humanosphere, Kyoto University, Gokasho, Uji, Kyoto 611-

5 0011, Japan

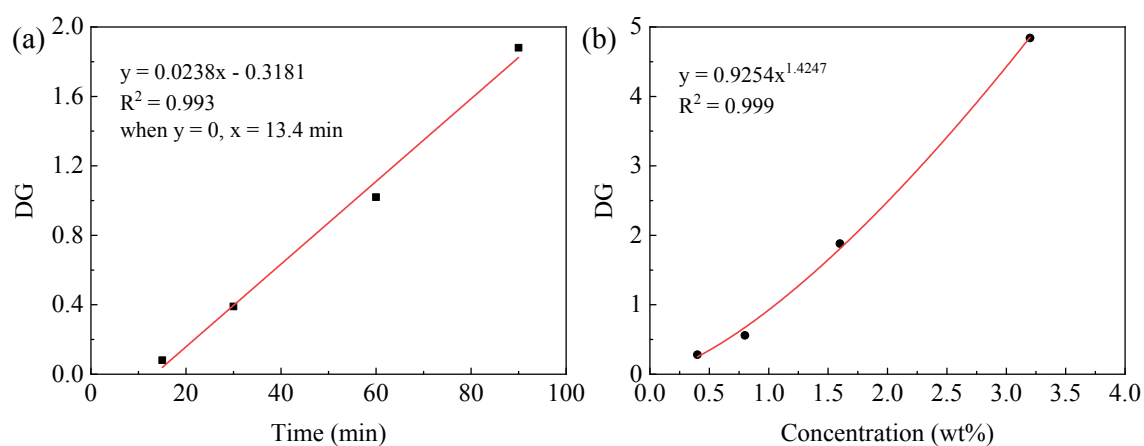
6 *Corresponding authors:

7 Xianpeng Yang: yang.xianpeng.84z@st.kyoto-u.ac.jp;

8 Kentaro Abe: abekentaro@rish.kyoto-u.ac.jp

9 The effect of polymerization time and monomer concentration on the DG

10 The purpose of this part is to reveal that the DG of CNF-g-PMMA was directly related to the
11 duration of the reaction and the concentration of the monomer. A linear fit (DG *versus* time) gave
12 an equation of $y = 0.0238x - 0.3181$ ($R^2 = 0.993$), suggesting that the DG increased linearly with
13 polymerization time. The x-intercept is 13.4 min. Therefore, we considered that there was an
14 induction period of current UV grafting and the value was approximately 13 min. In the case of
15 DG *versus* monomer concentration, a power function, $y = 0.9254x^{1.4247}$, fitted the data well. We
16 will determine the kinetics of UV grafting in the future study.



17
18

19 **Fig. S1** UV grafting of PMMA from the surfaces of CNFs. (a) DG as a function of polymerization
20 time. (b) DG as a function of monomer concentration.

21 Comparison of UV grafting with other methods

22 **Table S1.** Comparison of UV grafting with other polymer grafting methods concerning to CNF-g-PMMA

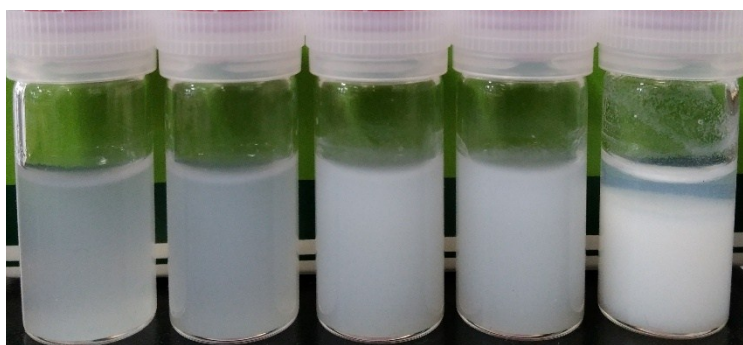
method	pre-treatment	polymerization condition	post-treatment	DG	homopolymer	Ref.
CAN initiation	None	0.2 wt% aqueous suspension, pH=1; CAN as initiator	centrifugation; washed with acetone and THF	0.6-1	25-44%	1
SI-ATRP	Immobilization of initiator in DMF	Bacterial cellulose membrane in DMF/H ₂ O; Cu(I)Br and PMDETA as catalyst	washed with DMF and water	0.59-8.87	none	2
UV grafting	None	0.2 wt% aqueous suspension; UV radiation	filtration	0.28-4.84	none	current work

23 THF: tetrahydrofuran; PMDETA: N,N,N',N'',N''-pentamethyldiethylenetriamine;

24 DMF: N, N-dimethylformamide

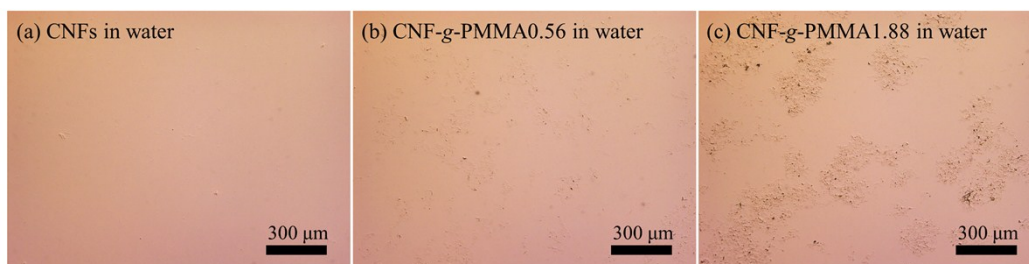
25 **As prepared CNF-g-PMMA suspensions**

26 After UV grafting, the as prepared CNF-g-PMMA suspensions look like homogeneous until the
27 DG reached 4.84 (Fig. S2). However, the microscope images showed that aggregation occurred
28 even the DS is low (Fig. S3). The aggregation of CNF-g-PMMA may facilitate the dewatering
29 which is an important issue for CNF materials.³



30

31 **Fig. S2** As prepared CNF-g-PMMA suspensions which were stored for one week. From left to right: CNF-
32 g-PMMA0.28, CNF-g-PMMA0.56, CNF-g-PMMA1.24, CNF-g-PMMA1.88 and CNF-g-PMMA4.84.

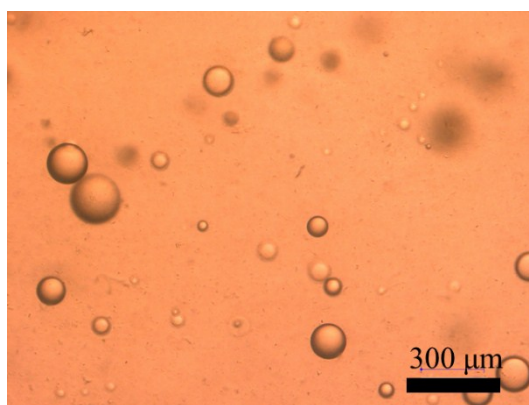


33

34 **Fig. S3** Microscope images of CNFs (a), CNF-g-PMMA0.56 (b) and CNF-g-PMMA1.88 (c).

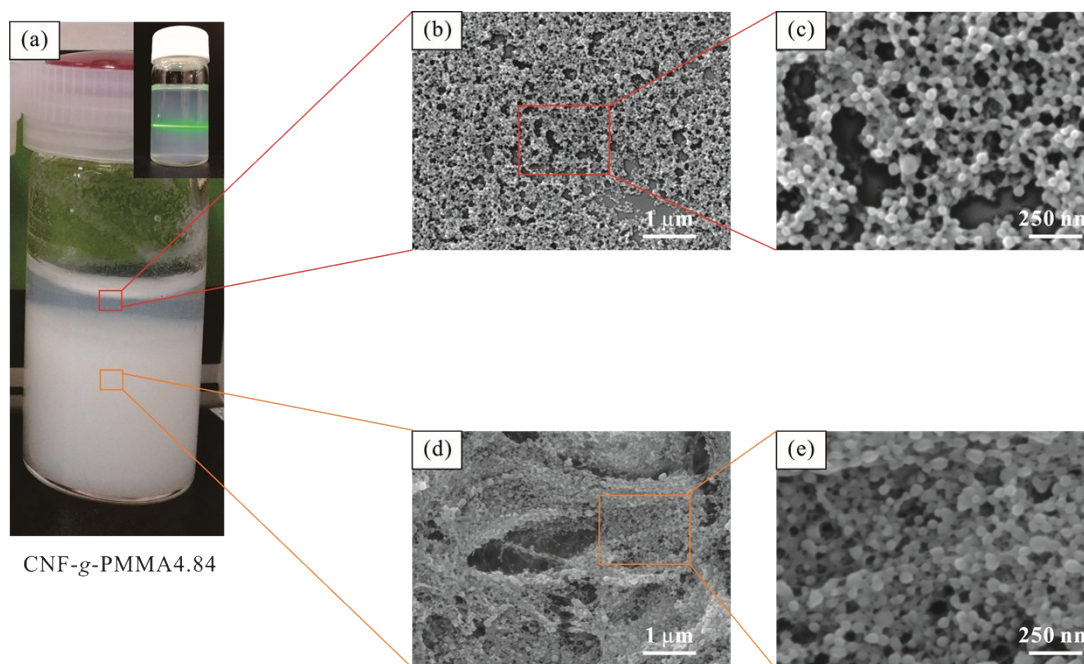
35 CNF-g-PMMA4.84

36 After UV grafting, the as prepared CNF-g-PMMA4.84 suspension separated, as shown in Fig.
37 S5a. Both the supernatant and sediments showed the nanofiber-nanoparticle structures (Fig. S5 b–
38 e). The supernatant had the same size as those of CNF-g-PMMA1.84 (Fig. S5c) while the
39 sediments showed increased size (Fig. S5e). However, we did not observe any PMMA
40 microparticles even in the image with lower magnification (Fig. S5d). Therefore, CNFs may be a
41 good template for preparation of unique nanostructures via UV grafting.



42

43 **Fig. S4** Microscope image of a CNF suspension containing 3.2 wt% MMA during UV grafting.



44

45 **Fig. S5** (a) As prepared CNF-g-PMMA4.84 suspension stored for one week. Inserted photo: the sediments
46 were diluted and ultrasonicated. (b–c) SEM images of the supernatant. (d–e) SEM images of the sediments.
47

48 **Chemical composition of CNFs**

49 Table S2 shows the chemical composition of CNFs used in the current study. The sugar
50 composition of the CNFs was determined from ion chromatography analysis after acid hydrolysis.
51 The hemicellulose is mainly glucomannan and xylan. The lignin content was measured by the
52 Klason lignin method.

53

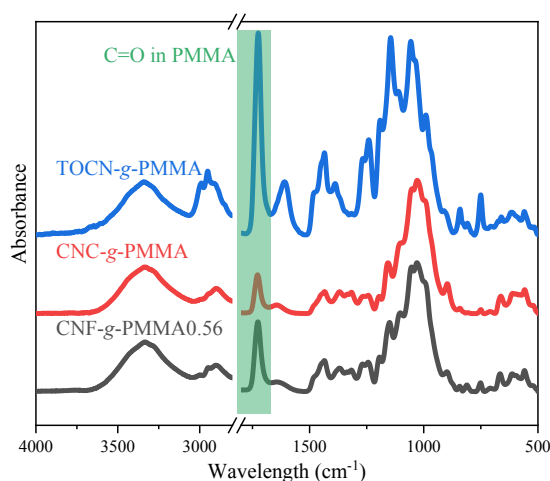
Table S2. Chemical composition of CNFs

sample	sugar composition with respect to total sugars, %					Klason content, %	lignin content, %
	glucose	mannose	xylose	galactose	arabinose		
CNFs	88.2	9.8	1.6	0.2	0.2	0.4	

54

55 UV grafting of other nanocelluloses

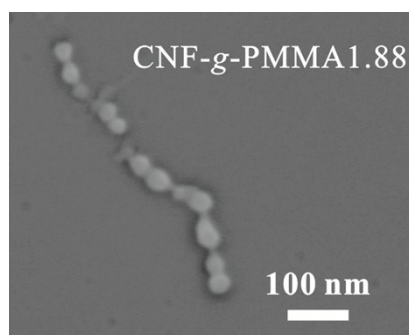
56 2,2,6,6-tetramethylpiperidine-1-oxyl radical-oxidized CNFs (TOCN) and cellulose nanocrystals
57 (CNCs) were used to the versatility of UV grafting for other nanocelluloses. Compared with the
58 CNFs, the hydrochloric acid hydrolyzed CNCs had higher crystallinity and less hemicellulose
59 content. On the other hand, TOCN had charged groups (COONa). During UV grafting, the
60 concentration of nanocellulose and MMA were 0.2 wt% and 0.8 wt%. Other conditions were the
61 same with the preparation of CNF-g-PMMA0.56. PMMA grafted TOCN (TOCN-g-PMMA) and
62 CNC (CNC-g-PMMA) were obtained (see FT-IR spectra in Fig. S6). The areas of the bands
63 ascribed to C=O of PMMA indicated that the reactivity was: TOCN > CNFs > CNCs.



64

65 **Fig. S6** FTIR spectra of the TOCN-g-PMMA, CNC-g-PMMA and CNF-g-PMMA0.56 samples, which
66 were normalized over the range 1316–1315 cm⁻¹.

67 Formation of PMMA nanoparticles



68

69 **Fig. S7** SEM image of CNF-g-PMMA1.88. The arrangement of PMMA nanoparticles in a line probably
70 implied that the particles grew around the surfaces of the CNFs after nucleation.

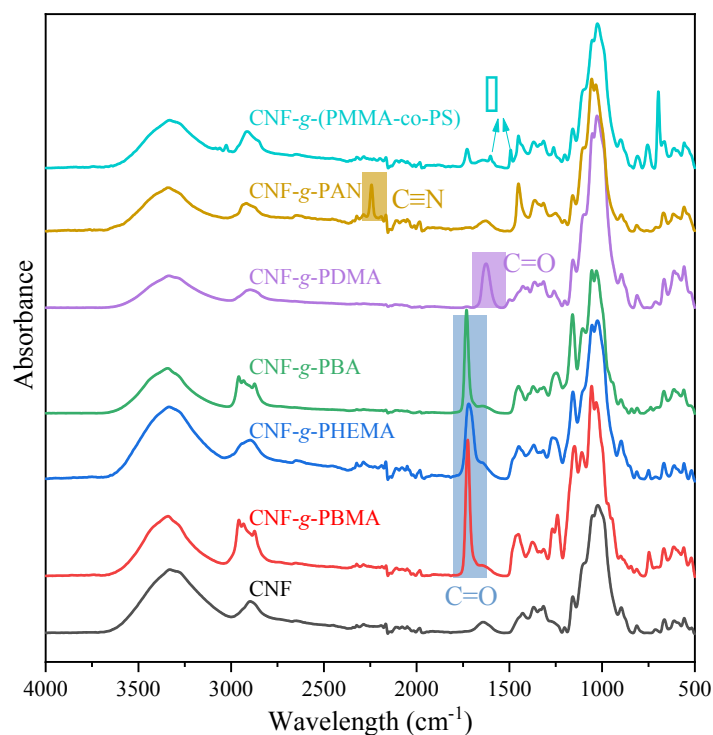
71 UV grafting of various polymers from the CNFs

72 Table S3 shows the UV grafting of various polymers from the CNFs. We can obtain polymer-
 73 grafted CNFs with different contact angles. Fig. S8 shows the FT-IR spectra of different polymers
 74 grafted CNFs. We also marked the characteristic bands of corresponding polymers in Fig. S8.

75 **Table S3.** UV grafting of various monomers from the CNFs and corresponding results

Monomers	conditions of polymerization				grafting degree	contact angle, °
	CNF, wt%	monomer, wt%	T, °C	t, min		
butyl methacrylate (BMA)	0.2	0.4	40	90	1.31	113.4 ± 1.1
2-hydroxyethyl methacrylate (HEMA)	0.2	0.4	40	90	0.59	75.7 ± 1.5
butyl acrylate (BA)	0.2	0.4	40	90	0.88	119.7 ± 1.5
N,N-dimethylacrylamide (DMA)	0.2	0.4	40	90	0.24	/
Acrylonitrile (AN)	0.2	7	40	720	2.1	64.3 ± 2.9
MMA-co-styrene	0.2	0.4-1.2	40	270	0.41	116.5 ± 1.2

76



77

78 **Fig. S8** FTIR spectra of the CNF, CNF-g-PBMA, CNF-g-PHEMA, CNF-g-PBA, CNF-g-PDMA, CNF-g-
 79 PAN and CNF-g-(PMMA-co-PS) samples, which were normalized over the range 1316–1315 cm^{-1} . PS:
 80 polystyrene.

81 **References**

- 82 1. Littunen, K.; Hippi, U.; Johansson, L.-S.; Österberg, M.; Tammelin, T.; Laine, J.;
83 Seppälä, J., Free radical graft copolymerization of nanofibrillated cellulose with acrylic
84 monomers. *Carbohydrate Polymers* **2011**, *84* (3), 1039-1047.
- 85 2. Lacerda, P. S.; Barros-Timmons, A. M.; Freire, C. S.; Silvestre, A. J.; Neto, C. P.,
86 Nanostructured composites obtained by ATRP sleeving of bacterial cellulose nanofibers
87 with acrylate polymers. *Biomacromolecules* **2013**, *14* (6), 2063-73.
- 88 3. Klemm, D.; Kramer, F.; Moritz, S.; Lindstrom, T.; Ankerfors, M.; Gray, D.; Dorris,
89 A., Nanocelluloses: a new family of nature-based materials. *Angew Chem Int Ed Engl*
90 **2011**, *50* (24), 5438-5466.

91